

Macroscopic quantum oscillations and controlled-NOT gate in superconducting qubits

Sam Young Cho¹ and Mun Dae Kim^{2,3,*}

¹Center for Modern Physics and Department of Physics,
Chongqing University, Chongqing 400044, China

²Institute of Physics and Applied Physics, Yonsei University, Seoul 120-749, Korea

³Korea Institute for Advanced Study, Seoul 130-722, Korea

(Dated: April 29, 2019)

We study the Rabi-type oscillation of superconducting flux qubit states, driven by a microwave threading the qubit loop. By using the non-resonant modes commensurate to the resonant mode of this Rabi-type oscillation, the controlled-NOT (CNOT) gate operations between weakly coupled qubits can be demonstrated. It is shown that by finely tuning the amplitude of microwave for any given coupling strength and qubit frequency the high fidelity for CNOT gate is achievable.

PACS numbers: 74.50.+r, 03.67.Lx, 85.25.Cp

Introduction.— The universal gate for quantum computing consists of the single qubit and the entangling two qubit operations. Usually the single qubit operations are driven by electromagnetic oscillations such as microwave, laser pulse, oscillating voltage and so on. The macroscopic spin state S_z of the NMR qubit [1] is driven by a magnetic field rotating in the x-y plane, which is described by the semi-classical Rabi oscillation. On the other hand, the atomic states of cavity-QED [2] and ion-trap [3] qubit, and the artificial atomic states of superconducting qubits such as the charge qubit employed in the circuit-QED quantum computing [4] and the flux qubit [5] are used as a natural basis of qubit states. In these cases the Rabi oscillation can be analyzed in the rotating wave approximation.

In this study we are considering the superconducting flux qubits. For superconducting flux qubits the magnetic flux threading qubit loop is directly coupled to the qubit energy levels and oscillating in z-direction, not rotating in x-y plane. The oscillation of the qubit states demonstrates a number of bumps which can be explained in a rotating frame. For a microwave resonant with the qubit frequency, the macroscopic current states of qubit is analyzed by the semi-classical Rabi oscillation in the rotating wave approximation. For some non-resonant microwaves, though the oscillation is far from the Rabi oscillation, the oscillation period can be commensurate with the Rabi-type oscillation. These commensurate modes take part in the controlled-NOT (CNOT) gate operation for two coupled qubits.

The CNOT gate is the most basic two-qubit operation for the universal gate [6]. Unfortunately, if the interaction between two qubits is weak, the CNOT gate performance is not satisfactory as desired [7]. In this paper, thus, we propose a scheme that can provide high fidelity for CNOT gate operation even for the weak interaction between qubits. When the oscillation periods of two coupled qubits are commensurate with each other, we found that the fidelity for the CNOT gate shows peaks of nearly the maximum value 1. These fidelity peaks can

be obtained for any interaction strength and any qubit frequency by finely-tuning the amplitude of oscillating magnetic field. The peak widths are sufficient for experimental realization. The present scheme is quite general, thus it can be applicable to other types of qubits.

Single flux qubit.— The Hamiltonian for a single three-Josephson junctions flux qubit under microwave irradiation (See Fig. 1(a)), $f_\omega(t) = (\Phi_{\text{mw}}/\Phi_0) \cos \omega t$, is given as $\mathcal{H} = \mathcal{H}_0 - \mathbf{M} \cdot \mathbf{B}(t)$, where $\mathcal{H}_0 = E_\downarrow |\downarrow\rangle\langle\downarrow| + E_\uparrow |\uparrow\rangle\langle\uparrow| - t_q (|\downarrow\rangle\langle\uparrow| + |\uparrow\rangle\langle\downarrow|)$, and $\mathbf{M} \cdot \mathbf{B}(t) = g \cos \omega t (|\downarrow\rangle\langle\downarrow| - |\uparrow\rangle\langle\uparrow|)$. Here $\Phi_{\text{mw}} = BS$ with the microwave magnetic field amplitude B and the area of the qubit loop S , $\Phi_0 = h/2e$ the superconducting unit flux quantum, $E_{\downarrow(\uparrow)}$ is the energy of diamagnetic (paramagnetic) current state of qubit loop, and t_q is the tunnelling rate between two qubit states. The coupling $g \equiv MB$ between the qubit and the microwave is given in terms of the magnetic moment M of qubit loop [8], where we set $M_\downarrow = -M_\uparrow \equiv M$.

The qubit energy levels $E_{\downarrow(\uparrow)}$ is controlled by the static external flux threading the qubit loop. At the degeneracy point $E_\downarrow = E_\uparrow = E_0$ the single qubit Hamiltonian can be expressed in transformed coordinates $|0\rangle = (|\downarrow\rangle + |\uparrow\rangle$

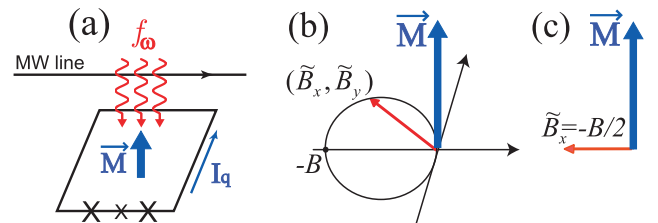


FIG. 1: (Color online) (a) A superconducting flux qubit with a microwave f_ω threading the qubit loop, which interacts with the magnetic moment M induced by the qubit current I_q . (b) The magnetic field \vec{B} of the microwave in the frame rotating with frequency ω . (c) The magnetic field \vec{B} in the rotating wave approximation.

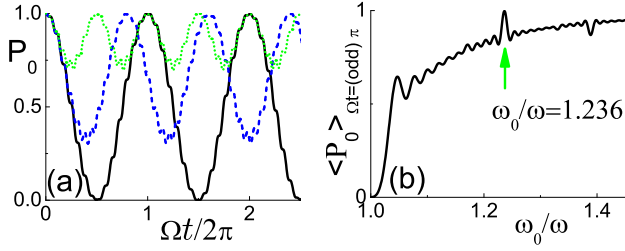


FIG. 2: (a) The oscillations of occupation probability P_0 for the state $|0\rangle$ with $\omega_0/\omega=1$ (solid), 1.1 (dashed), and 1.236 (dotted line). Here the initial state $\psi(0) = |0\rangle$, the qubit frequency $\omega_0/2\pi = 4.0\text{GHz}$, the oscillation frequency $\Omega \approx g/2\hbar$ and the coupling strength between qubit and microwave $g/h = 0.6\text{GHz}$. (b) Average of P_0 at $\Omega t = (\text{odd})\pi$. The peak at $\omega/\omega_0 = 1.236$ corresponds to the dotted line in (a).

$\rangle\rangle/\sqrt{2}$ and $|1\rangle = (|\downarrow\rangle - |\uparrow\rangle)/\sqrt{2}$ as

$$\mathcal{H} = -(\hbar\omega_0/2)\varrho_z + g \cos \omega t \varrho_x + E_0 I, \quad (1)$$

where $\hbar\omega_0 = 2t_q$ is the qubit frequency and $\varrho_{x,z}$ and I are the Pauli and identity matrix in the basis of $\{|0\rangle, |1\rangle\}$. With the resonant microwave, $\omega = \omega_0$, the qubit experiences a Rabi-type oscillation. In Fig. 2(a) we show the oscillation of occupation probability P_0 of state $|0\rangle$ (solid line) obtained numerically with the initial state $\Psi(0) = |0\rangle$. We found that the oscillation frequency is $\Omega \approx g/2\hbar$. For the non-resonant cases the qubit state cannot evolve to the state $|1\rangle$ completely (dashed and dotted lines).

These oscillations can be analyzed in an approximation. In coordinates rotating with the same frequency as the microwave frequency ω , the Schrödinger equation $\mathcal{H}\psi(t) = i\hbar\frac{\partial}{\partial t}\psi(t)$ is reexpressed as $i\frac{\partial}{\partial t}|\phi(t)\rangle = \tilde{\mathcal{H}}|\phi(t)\rangle$ by introducing $\phi(t) \equiv e^{-i\sigma_z\omega t/2}\psi(t)$. In this rotating frame the transformed Hamiltonian $\tilde{\mathcal{H}}$ is given by

$$\tilde{\mathcal{H}} = -\hbar(\omega_0 - \omega)\varrho_z - \tilde{B}_x M \varrho_x - \tilde{B}_y M \varrho_y \quad (2)$$

with $\tilde{B}_x(t) = -(B/2)(1 + \cos 2\omega t)$ and $\tilde{B}_y(t) = -(B/2)\sin 2\omega t$. This magnetic field shows a circular motion confined in the left half plane, $(\tilde{B}_x + B/2)^2 + \tilde{B}_y^2 = (B/2)^2$, in the rotating frame as shown in Fig. 1(b). The bumps in resonant oscillation [solid line in Fig. 2(a)] are attributed to this circular motion. These bumps are generated when the transformed magnetic field $\tilde{\mathbf{B}} = (\tilde{B}_x, \tilde{B}_y)$ completes a circular motion during the Rabi-type oscillation. Hence the number of bumps during a Rabi-type oscillation is given by the ratio $\omega_0/\Omega \approx 2\hbar\omega_0/g$.

In the limit of weak coupling between the qubit and the microwave, $\hbar\omega_0 \gg g$, there are huge number of negligibly small bumps, which produces a smooth Rabi oscillation for $\omega = \omega_0$. Naturally the high frequency modes, $\cos 2\omega_0 t$ and $\sin 2\omega_0 t$, of $\tilde{\mathbf{B}}$ -field can be neglected. In this approximation we can regard the circularly rotating magnetic field in Fig. 1(b) as a stationary one

$\tilde{B}_x = -B/2$ in Fig. 1(c). This dynamics of qubit states is essentially the same as the rotating wave approximation (RWA) for Jaynes-Cummings model [9], $H_{\text{JC}} = (1/2)\hbar\omega_0\varrho_z + \hbar\omega a^\dagger a + (g/2)(\varrho_+ + \varrho_-)(a + a^\dagger)$. By eliminating the terms, $\varrho_+ a^\dagger$ and $\varrho_- a$, which do not conserve energy, the model describes the quantum Rabi oscillation of cavity-QED [2] and ion-trap [3] qubit. In the semiclassical model of Eq. (1) for the macroscopic current states of flux qubits, this eliminating procedure maintains the term, $(g/2)(\varrho_+ e^{-i\omega t} + \varrho_- e^{i\omega t})$, which describes the Rabi oscillation by the magnetic field in Fig. 1(c).

In present case the coupling strength $g/\hbar\omega_0 \approx 0.15$ is relatively strong compared to that of quantum Rabi oscillation for cavity-QED and ion-trap qubit with $g/\hbar\omega_0 \approx 10^{-6} - 10^{-7}$. Nevertheless, we have found that RWA gives accurate results consistent with the numerical calculations. In RWA the oscillation frequency is given as

$$\Omega \equiv \sqrt{\left(\frac{\omega_0 - \omega}{2}\right)^2 + \left(\frac{g}{2\hbar}\right)^2}. \quad (3)$$

For the resonant microwave $\omega = \omega_0$, the frequency of Rabi oscillation is $\hbar\Omega_{\text{R}} = g/2$ as in Fig. 2(a).

When ω increases from the resonant value of ω_0 , the oscillation is not a Rabi-type oscillation between two qubit states any more [Fig. 2(a) dashed line]. Importantly, for specific values of ω the oscillation periods become commensurate with that of the resonant Rabi-type oscillation mode [Fig. 2(a) dotted line]. In Fig. 2(b) we show the averaged occupation probability $\langle P_0 \rangle$ at times $\Omega t = (\text{odd})\pi$, which demonstrates a sharp peak of $\langle P_0 \rangle$ close to 1. This commensurate mode cannot be used for a single qubit operation, but can play an important role in two-qubit CNOT gate operation.

CNOT gate with a weak coupling.— In order to achieve a CNOT gate with high fidelity, in general a sufficiently

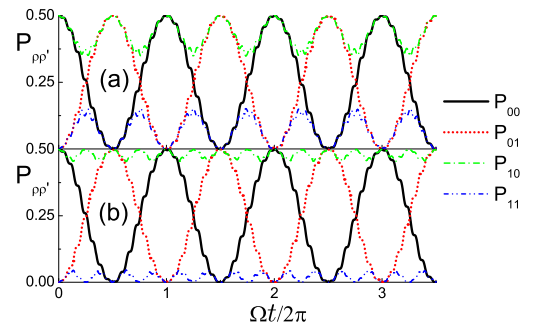


FIG. 3: (Color online) (a) Occupation probability oscillations of coupled-qubit states with the initial state, $|\psi(0)\rangle = (|0_\alpha 0_\beta\rangle + |1_\alpha 0_\beta\rangle)/\sqrt{2}$. The non-resonant oscillation modes with P_{10} and P_{11} are commensurate with the resonant modes with P_{00} and P_{01} . At $\Omega t = (\text{odd})\pi$, P_{10} and P_{11} recover their initial values, thus the CNOT gate operations can be achieved with high fidelity. Here the coupling strength $J/h = 0.76\text{GHz}$, $\omega_0/2\pi = 4.0\text{GHz}$ and $g/h = 0.6\text{GHz}$. (b) Higher order commensurate modes with $J/h = 1.22\text{GHz}$.

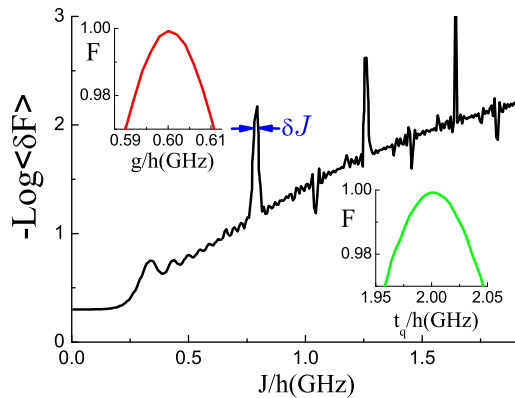


FIG. 4: (Color online) Deviation of fidelity, $\delta F = 1 - F$, for CNOT gate shows peaks, where the first and second peaks correspond to the commensurate modes in Fig. 3(a) and (b), respectively. The width of first fidelity peak for $J/h = 0.76$ GHz is $\delta J/h \approx 0.017$ GHz. Insets show the fidelity envelop for the first peak as a function of g and t_q .

strong coupling between qubits is required [8, 10]. The control qubit state should remain unchanged, while the target qubit evolves between qubit states. Unfortunately, if the coupling is weak, the control as well as the target qubit also evolves in time. In this study we discuss how the high performance of CNOT gate would be achieved even though the coupling is weak, if the control qubit oscillation is one of the above commensurate modes.

Two inductively coupled flux qubits (qubit α and β) are described by the Hamiltonian $\mathcal{H} = \mathcal{H}_\alpha \otimes I + I \otimes \mathcal{H}_\beta + J\sigma_z^\alpha \otimes \sigma_z^\beta$, where σ_z is the Pauli matrix in the basis of $\{|\downarrow\rangle, |\uparrow\rangle\}$ and $J = \mathcal{M}I_q^\alpha I_q^\beta = (\mathcal{M}/S^2)M^\alpha M^\beta$ is the coupling strength with the mutual inductance \mathcal{M} between the two qubits. The energy levels of coupled qubit states, $|s_\alpha s'_\beta\rangle$ with $s \in \{\downarrow, \uparrow\}$, are given by $E_{ss'} = E_s^\alpha + E_{s'}^\beta + (\mathcal{M}/S^2)M_s^\alpha M_{s'}^\beta$, where we set $M_\downarrow^{\alpha(\beta)} \approx -M_\uparrow^{\alpha(\beta)} \equiv M^{\alpha(\beta)}$. We adjust the external static fluxes in a way that the control qubit (say, qubit α) is far away from the degeneracy point, and the target qubit (qubit β) is at a degeneracy point such that $E_{\uparrow\uparrow} > E_{\uparrow\downarrow} > E_{\downarrow\downarrow} = E_{\downarrow\uparrow}$. Then the tunneling process t_q^β of qubit β takes a role, while t_q^α is negligible due to the energy level difference. Here we introduce a coordinate transformation, $|s_\alpha 0_\beta\rangle = (|s_\alpha \downarrow_\beta\rangle + |s_\alpha \uparrow_\beta\rangle)/\sqrt{2}$ and $|s_\alpha 1_\beta\rangle = (|s_\alpha \downarrow_\beta\rangle - |s_\alpha \uparrow_\beta\rangle)/\sqrt{2}$. Moreover, since there is no tunnelling in qubit α , we can set $|\downarrow_\alpha\rangle \approx |0_\alpha\rangle$ and $|\uparrow_\alpha\rangle \approx |1_\alpha\rangle$, and thus $|\downarrow_\alpha 0_\beta\rangle \approx |0_\alpha 0_\beta\rangle$, $|\downarrow_\alpha 1_\beta\rangle \approx |0_\alpha 1_\beta\rangle$, $|\uparrow_\alpha 0_\beta\rangle \approx |1_\alpha 0_\beta\rangle$, and $|\uparrow_\alpha 1_\beta\rangle \approx |1_\alpha 1_\beta\rangle$.

Therefore, the Rabi-type oscillation can take place between the states of qubit β , $|0_\beta\rangle$ and $|1_\beta\rangle$, which is described by the Hamiltonian

$$\mathcal{H} = \sum_{\rho=0,1} \left[\mathcal{E}_{\rho 0} |\rho 0\rangle \langle \rho 0| + \mathcal{E}_{\rho 1} |\rho 1\rangle \langle \rho 1| \right]$$

$$+ M^\beta B \cos \omega t (|\rho 0\rangle \langle \rho 1| + |\rho 1\rangle \langle \rho 0|). \quad (4)$$

Here the energy gaps are $\hbar\omega_0 = \mathcal{E}_{01} - \mathcal{E}_{00} = 2t_q$ and $\hbar\omega_1 = \mathcal{E}_{11} - \mathcal{E}_{10} = 2\sqrt{[(E_{\uparrow\uparrow} - E_{\uparrow\downarrow})/2]^2 + t_q^2}$, and the coupling strength is given by $J = \frac{1}{4}(E_{\downarrow\uparrow} + E_{\uparrow\downarrow} - E_{\downarrow\downarrow} - E_{\uparrow\uparrow})$ [10, 11]. Since $E_{\downarrow\downarrow} = E_{\downarrow\uparrow}$ at this operating point, we get

$$\hbar\omega_1 = 2\sqrt{(2J)^2 + t_q^2}. \quad (5)$$

For a negligible coupling $J \approx 0$, $\omega_0 \approx \omega_1$. Indeed, the resonant microwave $\omega = \omega_0$ inducing a Rabi-type oscillation between $|0_\alpha 0_\beta\rangle$ and $|0_\alpha 1_\beta\rangle$ also invokes a oscillation between $|1_\alpha 0_\beta\rangle$ and $|1_\alpha 1_\beta\rangle$. That is to say, the resonant microwave in this case cannot discriminate the control qubit state $|0_\alpha\rangle$ from $|1_\alpha\rangle$. Hence we cannot expect CNOT gate operation. However, if J is much larger than t_q , the states $|1_\alpha 0_\beta\rangle$ and $|1_\alpha 1_\beta\rangle$ will not respond to this microwave. For inductively coupled flux qubits [7, 12], usually $J = (0.5 \sim 1)$ GHz while t_q is of the order of GHz.

Our scheme we propose here is to use the oscillations of $|1_\alpha 0_\beta\rangle$ and $|1_\alpha 1_\beta\rangle$ states which are commensurate with the oscillations of $|0_\alpha 0_\beta\rangle$ and $|0_\alpha 1_\beta\rangle$. In Fig. 3 we show two examples of such commensurate modes. The initial state, $|\psi(0)\rangle = (|0_\alpha 0_\beta\rangle + |1_\alpha 0_\beta\rangle)/\sqrt{2}$, evolves owing to the resonant microwave $\omega = \omega_0 < \omega_1$. By varying the coupling strength J with the fixed qubit frequency ω_0 and amplitude of microwave B , we were able to find a resonant behavior; the oscillation period of the $|0_\alpha 0_\beta\rangle$ and $|0_\alpha 1_\beta\rangle$ states is a multiple of that of the $|1_\alpha 0_\beta\rangle$ and $|1_\alpha 1_\beta\rangle$ states

The CNOT gate operation occurs when the occupation probability P_{00} (P_{01}) is reversed perfectly from 0.5 (0) to 0 (0.5) at $\Omega t = (\text{odd})\pi$. At the same time, we can observe that the probabilities P_{10} and P_{11} recover their initial values 1 and 0, respectively. As a result, the CNOT operation is achieved with a good performance at this coupling strength. As the coupling increases further, another resonance with a shorter period appears (Fig. 3(b)). Actually we have found a series of commensurate modes as J increases.

The fidelity for CNOT gate operation is given by $F(t) = \text{Tr}(M(t)M_{\text{CNOT}})/4$, where M_{CNOT} is the matrix for the perfect CNOT operation and $M(t)$ is the truth table amplitude at time t [7]. In Fig. 4 we show the deviation of fidelity, $\delta F = 1 - F$, from the maximum value 1 as a function of J . Here $\langle \delta F \rangle$ is the averaged values of δF over 10 points of $(\text{odd})\pi$ in Fig. 3. In Fig. 4 we see series of peaks: 1st and 2nd peaks correspond to the CNOT operation in Fig. 3(a) and (b), respectively. They show that the errors can be small as much as $10^{-2} \sim 10^{-3}$, which is very close to the fault tolerant quantum computing. In Fig. 4 the dip between peaks appears at the anti-resonant points, where P_{10} (P_{11}) has minimum (maximum) at $\Omega t = (\text{odd})\pi$.

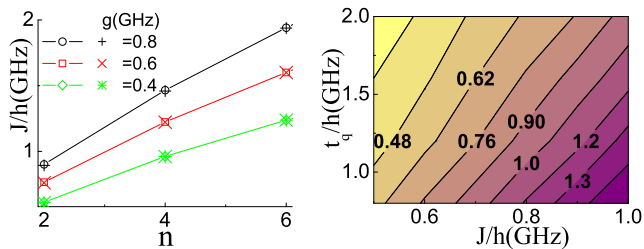


FIG. 5: (Color online) (a) The values of coupling strength J at peak positions for various g . The lines with open marks show the values obtained from Eq. (6) and the scattered marks from the numerical calculation. Here we set $t_q/h = 2$ GHz. (b) The values of g (GHz) obtained numerically at the first fidelity peak corresponding to $n = 2$ of Eq. (7) in (J, t_q) plane.

For the first peak at $J/h = 0.76$ GHz we found that the peak width at $\delta F = 10^{-2}$ is $\delta J/h \approx 0.017$ GHz, which is within controllability range of experimental situations. Since for second, third or higher peaks the difference between ω_0 and ω_1 increases, the peak width becomes narrower. Thus in following analysis we concentrate on the first peak. In fact, there also exist fluctuations of other variables. In the insets of Fig. 4 the envelopes of fidelity are shown as functions of magnetic field amplitude $B = g/M$ and qubit frequency t_q . For these cases we observe that $\delta g/h \approx 0.01$ GHz and $\delta t_q/h \approx 0.05$ GHz at $\delta F = 10^{-2}$, which is the same order of δJ .

By using the RWA we can analyze the condition for the commensurate modes. The control and target qubit can approximately be considered to oscillate with frequencies $\Omega_1 = \sqrt{\left(\frac{\omega_0 - \omega_1}{2}\right)^2 + \left(\frac{g}{2\hbar}\right)^2}$ and $\Omega_0 = g/2\hbar$, respectively, from Eq. (3). Then the resonant condition is given by

$$n \frac{2\pi}{\Omega_1} = \frac{2\pi}{\Omega_0}. \quad (6)$$

When integer n is even, we can obtain the values J for peaks in Fig. 4 by using Eq. (5), while for odd $n > 1$ the dips appear. In Fig. 5(a) we compare the numerical values of J at peak points with those in the RWA, which shows that two values fit well with each other. The approximate values are a little higher than the numerical values and the small deviation tends to increase along with g .

In experimental situations usually the coupling J and the qubit frequency t_q are fixed in the beginning, thus the control of magnetic field amplitude B with fixed J and t_q will be more desirable. For any given pair of (J, t_q) , in principle, we can find a commensurate oscillation by finely tuning the value of B . From Eq. (6) the value of $g = MB$ for fidelity peaks can be expressed as

$$g = \frac{2}{\sqrt{n^2 - 1}} \left(\sqrt{4J^2 + t_q^2} - t_q \right). \quad (7)$$

In Fig. 5(b) we show g obtained numerically, corresponding to the first peak with $n = 2$ in Eq. (7). The value of

B should increase, as J increases and t_q decreases. This is consistent with Eq. (7). Also it can be understood in conjunction with Eq. (3) which describes the rotation with Eq. (3) which describes the rotation about the z-axis. For the resonant condition $\omega = \omega_0$ we expect the rotation about x-axis, i.e., a Rabi-type oscillation. The commensurate oscillation in Fig. 3(a) occurs for a specific value of θ . Hence, when ω_1 increases (or ω_0 decreases), B should also increase to preserve the specific value of θ . Hence, if we tune the amplitude of microwave, the high fidelity CNOT gate operation can be achieved for a given values of qubit frequency t_q and two-qubit coupling strength J in an experimental setup.

Summary.— We study the operation of flux qubits driven by a oscillating microwave field, where the oscillating magnetic flux is directly coupled to the qubit energy levels. The non-resonant modes, but commensurate to the resonant mode, make it possible to achieve the CNOT gate operation even for weak coupling between qubits. We show that the fidelity envelopes around the peak points have sufficiently wide width for experimental realization. For given values of qubit frequency and coupling between qubits, the amplitude of microwave for the CNOT gate operation can be calculated. Therefore, by finely tuning of the microwave amplitude around this value the high performance CNOT gate for a weak coupling will be realized.

* Corresponding author; E-mail address: mdkim@kias.re.kr

- [1] D. G. Cory, A. F. Fahmy, and T. F. Havel, Proc. Natl. Acad. Sci. U.S.A. **94**, 1634 (1997); N. A. Gershenfeld and I. L. Chuang, Science **275**, 350 (1997); L. M. K. Vanderspen and I. L. Chuang, Rev. Mod. Phys. **76**, 1037 (2004).
- [2] J. M. Raimond, M. Brune, and S. Haroche, Rev. Mod. Phys. **73**, 565 (2001).
- [3] J. I. Cirac and P. Zoller, Phys. Rev. Lett. **74**, 4091 (1995).
- [4] A. Blais, R. S. Huang, A. Wallraff, S. M. Girvin, and R. J. Schoelkopf, Phys. Rev. A **69**, 062320 (2004); A. Wallraff, D. I. Schuster, A. Blais, L. Frunzio, R. S. Huang, J. Majer, S. Kumar, S. M. Girvin, and R. J. Schoelkopf, Nature (London) **431**, 162 (2004).
- [5] J. E. Mooij *et al.*, Science **285**, 1036 (1999); C. H. van der Wal *et al.*, Science **290**, 773 (2000); I. Chiorescu *et al.*, Science **299**, 1869 (2003).
- [6] A. Barenco *et al.*, Phys. Rev. A **52**, 3457 (1995).
- [7] J. H. Plantenberg, P. C. de Groot, C. J. P. M. Harmans, and J. E. Mooij, Nature **447**, 836 (2007).
- [8] M. D. Kim and S. Y. Cho, *unpublished*.
- [9] E. T. Jaynes and F. W. Cummings, Proc. IEEE **51**, 89 (1963).
- [10] M. D. Kim and J. Hong, Phys. Rev. B **70**, 184525 (2004).
- [11] M. D. Kim, Phys. Rev. B **74**, 184501 (2006).
- [12] J. B. Majer, F. G. Paauw, A. C. J. ter Haar, C. J. P. M. Harmans, and J. E. Mooij, Phys. Rev. Lett. **94**, 090501 (2005); T. Hime *et al.*, Science **314**, 1427 (2006); A. O. Niskanen *et al.*, Science **316**, 723 (2007).